Integrins protect sensory neurons in models of paclitaxel-induced peripheral sensory neuropathy

Grace Ji-eun Shin[a,1], Maria Elena Pero[b,c], Luke A. Hammond[a], Anita Burgos[a], Atul Kumar[b], Samantha E. Galindo[a], Tanguy Lucas[a], Francesca Bartolini[b], and Wesley B. Grueber[a,d,e]

[a]Zuckerman Mind Brain Behavior Institute, Jerome L. Greene Science Center, Columbia University, New York, NY 10027; [b]Pathology & Cell Biology, Columbia University, New York, NY 10032; [c]Department of Veterinary Medicine and Animal Production, University of Naples Federico II, 80137, Naples, Italy; [d]Physiology and Cellular Biophysics, Columbia University, New York, NY 10032; and [e]Neuroscience, Columbia University, New York, NY 10027

Edited by David D. Ginty, Harvard Medical School, Boston, MA, and approved February 24, 2021 (received for review April 19, 2020)

Chemotherapy-induced peripheral neuropathy (CIPN) is a major side effect from cancer treatment with no known method for prevention or cure in clinics. CIPN often affects unmyelinated nociceptive sensory terminals. Despite the high prevalence, molecular and cellular mechanisms that lead to CIPN are still poorly understood. Here, we used a genetically tractable *Drosophila* model and primary sensory neurons isolated from adult mouse to examine the mechanisms underlying CIPN and identify protective pathways. We found that chronic treatment of *Drosophila* larvae with paclitaxel caused degeneration and altered the branching pattern of nociceptive neurons, and reduced thermal nociceptive responses. We further found that nociceptive neuron-specific overexpression of integrins, which are known to support neuronal maintenance in several systems, conferred protection from paclitaxel-induced cellular and behavioral phenotypes. Live imaging and superresolution approaches provide evidence that paclitaxel treatment causes cellular changes that are consistent with alterations in endosome-mediated trafficking of integrins. Paclitaxel-induced changes in recycling endosomes precede morphological degeneration of nociceptive neuron arbors, which could be prevented by integrin overexpression. We used primary dorsal root ganglia (DRG) neuron cultures to test conservation of integrin-mediated protection. We show that transduction of a human integrin β-subunit 1 also prevented degeneration following paclitaxel treatment. Furthermore, endogenous levels of surface integrins were decreased in paclitaxel-treated mouse DRG neurons, suggesting that paclitaxel disrupts recycling in vertebrate sensory neurons. Altogether, our study supports conserved mechanisms of paclitaxel-induced perturbation of integrin trafficking and a therapeutic potential of restoring neuronal interactions with the extracellular environment to antagonize paclitaxel-induced toxicity in sensory neurons.

CIPN | neuropathy | integrins | cell surface proteins | *Drosophila*

Chemotherapy-induced peripheral neuropathy (CIPN) is a prevalent adverse effect of treatment in cancer patients and survivors (1). CIPN significantly impacts quality of life as damage to sensory nerves may be permanent, and is often a dose-limiting factor during cancer treatment (2–4). Patients with CIPN report pain-related symptoms, including allodynia, hyper- or hypoalgesia, or pain that can be more severe than the pain associated with the original cancer (4). Despite increasing data on agents that protect sensory nerves, our limited understanding of the mechanisms of CIPN impedes effective treatment (5). Studies from model systems may be helpful in identifying molecules that protect sensory neuron morphology and function from the effects of chemotherapeutics.

In the present study, we explored the mechanisms of CIPN induced by paclitaxel using two established models: *Drosophila* larval nociceptive neurons (6, 7) and primary dorsal root ganglia (DRG) neurons isolated from adult mouse (8). Similar to other peripheral neuropathies, CIPN models using paclitaxel, bortezomib, oxaliplatin, and vincristine report changes in unmyelinated intraepidermal nerve fibers (IENFs) that detect painful or noxious stimuli (9–14). These small fibers are embedded in the epidermis, and continuously turn over coincident with the turnover of skin (9, 15). *Drosophila* class IV nociceptive neurons are a favored model for genetic studies of nociceptive neuron development and signaling mechanisms (16). Prior studies showed that class IV neuron morphology is sensitive to paclitaxel and demonstrated morphological changes of nociceptive neurons at the onset and the end stage of paclitaxel-induced pathology (6, 7). Specifically, chronic treatment of high doses (30 μM) induce fragmentation and simplification of branching of sensory terminals (6). Additionally, acute treatments of moderate doses (10 to 20 μM) induced hyperbranching of sensory arbors without changing the branch patterns or degeneration (7). Nociceptive neurons in *Drosophila* larvae detect multiple qualities of noxious stimuli (17, 18), and project naked nerve terminals that are partially embedded in the epidermis (19, 20). Larvae have a stereotyped behavioral response toward noxious stimuli that can serve as a readout of nociceptive neuron function (17, 21). Nociceptive neurons in *Drosophila* larvae may therefore serve as a good in vivo model to study morphological and functional changes to sensory neurons induced by chemotherapeutics.

Paclitaxel binds to tubulin and prevents microtubule disassembly. It is a commonly used chemotherapeutic drug for treatment of solid cancers, such as breast, ovarian, and lung cancers, by virtue of its ability to inhibit cell division. Paclitaxel causes chronic sensory neuropathy in patients and animal models (22–24). Several CIPN animal and in vitro models have also revealed acute effects

Significance

Paclitaxel is a common chemotherapeutic agent and often causes a form of sensory dysfunction termed chemotherapy-induced peripheral neuropathy (CIPN). There is no approved therapy to counteract CIPN, although the CIPN symptoms interfere with effective cancer treatment and impose long-term health and economic burdens for cancer survivors. As chemotherapy is still a first-line treatment for many patients, understanding the basis for CIPN is critical. Using complementary approaches in *Drosophila* and mouse sensory neurons, we characterized paclitaxel-induced cellular and behavioral changes. We link changes in sensory neurons with integrins, cell surface receptors critical for coupling neurons with the extracellular matrix. Altogether, we propose that altered interactions between sensory neurons and their extracellular environment are an important contributor to paclitaxel-induced peripheral neuropathy.

Author contributions: G.J.-e.S. and W.B.G. designed research; G.J.-e.S., M.E.P., A.B., A.K., and S.E.G. performed research; G.J.-e.S., L.A.H., and T.L. contributed new reagents/analytic tools; G.J.-e.S., M.E.P., L.A.H., A.B., S.E.G., F.B., and W.B.G. analyzed data; and G.J.-e.S. and W.B.G. wrote the paper.

The authors declare no competing interest.

This article is a PNAS Direct Submission.

[1]To whom correspondence may be addressed. Email: js4920@columbia.edu.

This article contains supporting information online at https://www.pnas.org/lookup/suppl/doi:10.1073/pnas.2006050118/-/DCSupplemental.

Published April 5, 2021.

of paclitaxel (7, 8, 24–26). While the mechanisms of acute and chronic neurodegeneration are likely to be distinct (27), how long-term treatment of paclitaxel can affect sensory neuron morphology and function, and how neuronal arbors can be protected against long-term toxicity is not understood.

Several studies have shown that nociceptive sensory terminals share a close relationship with specific extracellular structures, most notably epidermal cells and the extracellular matrix (ECM). Thus, in addition to direct effects on neurons, paclitaxel could conceivably destabilize terminals by disrupting relationships with the extracellular environment. Indeed, a study in zebrafish indicates that epidermal cells are directly affected by paclitaxel and that epidermal changes precede neuronal degradation, indicating that degradation of neuronal substrates contributes to degeneration of adjacent arbors (25). For the most part, however, extracellular contributions to neuropathy induced by chemotherapeutics are still poorly characterized. It is therefore important to determine how sensory terminals are maintained in the context of a dynamic extracellular environment that itself may be sensitive to chemotherapeutics. Integrins are a key mediator of the interaction between cells and the ECM, and impact dendrite stabilization and maintenance in both vertebrate and invertebrate systems (20, 28, 29). Prior studies in other systems indicate that integrin levels at the surface are maintained by continuous recycling via tight regulation of the endosomal pathway rather than degradation and de novo synthesis (30). Decreased recycling or increased degradation could lead to depletion of the surface receptors (31, 32) responsible for arbor maintenance and, in turn, degeneration of nociceptive terminals. We therefore explored whether integrin–ECM interactions may impact sensory neuron maintenance upon paclitaxel-induced toxicity and how the endosomal–lysosomal pathway may be linked to the maintenance of sensory neurons.

Here, we have used *Drosophila* and isolated mouse DRG neurons to investigate the pathological effect of paclitaxel in sensory neurons. Morphological changes in *Drosophila* neurons occurred at paclitaxel doses that also caused changes in thermal nociceptive behaviors. Cell-specific overexpression of integrins protected nociceptive neurons from morphological alterations and prevented the thermal nociceptive behavior deficits caused by paclitaxel in *Drosophila*. Transduction of integrins also protected adult mouse DRG sensory neurons from paclitaxel-induced toxicity in vitro, indicating that integrin-mediated protection is conserved in a vertebrate model of CIPN. We provide evidence that paclitaxel alters intracellular trafficking in both *Drosophila* and mouse models of CIPN. Furthermore, our biochemical analysis indicates a reduction of integrin surface availability, suggesting paclitaxel-induced recycling defects in mouse DRG neurons in vitro. Our study suggests that altered interactions between sensory neurons and their extracellular environment are an important contributor to paclitaxel-induced neuronal pathology, and that preventing these changes may offer a therapeutic approach.

Results

Paclitaxel Alters the Branching Pattern of *Drosophila* Nociceptive Neurons. We first sought to confirm and extend prior results on the effect of paclitaxel on *Drosophila* sensory dendrites using high-resolution analysis of terminal morphology. We administered paclitaxel (10, 20, and 30 μM) in food beginning from 24 to 28 h after egg laying (AEL; early first instar). By this stage, dendritic arborization (da) sensory neurons have completed axon pathfinding and formed major peripheral dendrite branches (33). All of these paclitaxel concentrations were previously used as models for CIPN (6, 7). We dissected treated larvae at the late third-instar stage. Survival of larvae treated with 30 μM was rare (<5% survival rate by third instar stages), but animals tolerated 10 and 20 μM well and often survived past third instar stages. The da neuron branches still broadly covered their territories in larvae fed 10 and 20 μM (Fig. 1 *A*–*C*), but neurons showed clear morphological changes, such as predegenerative varicosities and fragmentation resembling phenotypes reported in vertebrate models (9, 24) (Fig. 2 and *SI Appendix*, Fig. S1). Nociceptive neurons in animals treated with 10 μM did not show an overt change in branching pattern. In contrast, 20-μM treatments induced marked changes in branching patterns (Fig. 1 *D*, *E*, and *G*). Peripheral arbors were sporadically clumped and patchy in proximal regions of the arbor and depleted in more distal regions (Figs. 1 *A*–*C*, 2 *A*, *C*, and *C'*, and *SI Appendix*). We developed an analysis to compare branch density and how density is distributed across the dendritic field. Density analysis revealed that control nociceptive arbors have a clear maximal peak density, indicating a relatively even and uniform field coverage (Fig. 1*D* and *SI Appendix*, Fig. S2*A*).

In contrast, paclitaxel dose-dependently increased overall local density of nociceptive arbors and the density distribution lacked a clear peak (Fig. 1*D* and *SI Appendix*, Fig. S2 *B* and *C*). Thus, paclitaxel treatment leads to a more heterogeneous distribution of dendrites. By plotting density according to the distance from soma, we found that paclitaxel caused an increase in proximal branch density (Fig. 1*E*), which was also supported by Sholl analysis (*SI Appendix*, Fig. S2*E*). Neither concentration of paclitaxel caused a change in total dendrite length compared to control (Fig. 1*F*). In contrast, we found that 20 μM caused a robust increase in the number of total dendrite branch points ($P < 0.001$), compared to a modest increase observed with 10-μM treatment ($P = 0.106$) (Fig. 1*G*). Thus, to explore the events that may precede degeneration of nociceptive arbors, we used both 10 and 20 μM, and used 20 μM of paclitaxel to further study the effects on nociceptive arbor branching pattern and degenerative changes.

Paclitaxel-Induced Changes Are Prevented by Cell-Specific Integrin Overexpression in Nociceptive Sensory Neurons. In addition to causing degeneration in nociceptive neurons, paclitaxel feeding resulted in extensive branch crossing of cIV dendrites, indicating a failure of self-avoidance (Fig. 2 *A*, *C*, *C'*, *E*, and *F*). Two parallel mechanisms impact self-avoidance in *Drosophila* sensory dendrites. Dscam1-mediated recognition between sister dendrites results in repulsion and avoidance (34–36). In parallel, integrin receptors for the ECM maintain dendrites in a mostly two-dimensional (2D) arrangement on the epidermis by mediating substrate attachment (19, 20). This placement ensures that dendrites come into contact with one another as they grow, rather than grow over or under each other in 3D (19, 20). The observed defect in self-avoidance caused by paclitaxel raised the possibility that paclitaxel disrupts one of these mechanisms that prevent dendrite crossing. Consistent with this hypothesis, cooverexpression of αPS1 and βPS integrins in nociceptive neurons lessened paclitaxel-induced dendrite crossing (Fig. 2 *B*, *D*, *D'*, and *E*). These data suggest that paclitaxel compromises the link between dendrite processes and the ECM, which can be compensated by increased levels of integrins.

Remarkably, integrin overexpression also largely rescued paclitaxel-induced degenerative phenotypes (Fig. 2 *D*, *D'*, and *F*). We compared this result with another cell adhesion receptor, N-cadherin, which is known to promote cellular growth through cell–cell interactions (37, 38). We found that N-cadherin overexpression in nociceptive neurons partially prevented paclitaxel-induced phenotypes but not to the same degree as integrins (*SI Appendix*, Fig. S3). These results raise the possibility that integrin-mediated attachment to the ECM substrate and, to a lesser degree, cell–cell interactions through N-cadherin, can counterbalance the effects of paclitaxel treatment.

Integrin Overexpression Prevents Paclitaxel-Induced Change in a Thermal Nociceptive Response. *Drosophila* larvae show a stereotyped nocifensive escape behavior in response to thermal or mechanical noxious stimuli. The escape sequence consists of C-shaped body bending, lateral rolling, and fast escape crawl (17, 21, 39, 40). To examine whether paclitaxel disrupts nocifensive responses, we

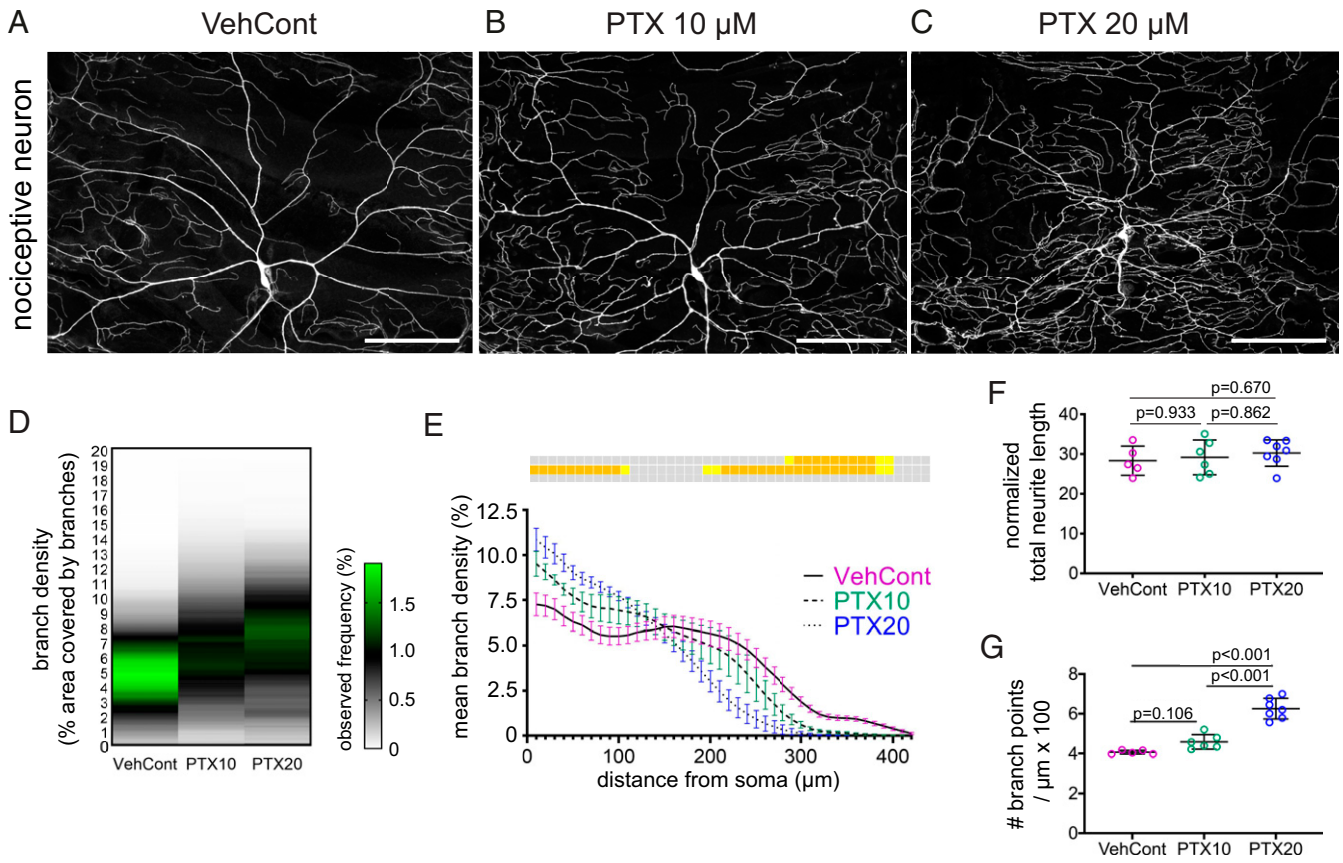

Fig. 1. Paclitaxel causes changes in nociceptive neuron branch pattern in *Drosophila*. (*A*–*C*) Confocal micrographs from animals fed with vehicle control (VehCont, *A*) and two different concentrations of paclitaxel [PTX; 10 μM (*B*) and 20 μM (*C*)], harboring a nociceptive neuron driver and a marker (*ppk1.9Gal4*, *ppkcd4tdgfp*). Data were collected from two independent experiments per condition, and a single cell was quantified per animal. (Scale bars, 100 μm.) (*D* and *E*) Density analyses of animals treated with VehCont ($n = 7$) and two different concentrations of PTX (10 and 20 μM, $n = 6$ and 7, respectively). Branch density is calculated as described in *SI Appendix, SI Materials and Methods* and Fig. S2. The same data are used in *D* and *E* except data in *E* are plotted according to distance from the neuronal soma. Mean of each segment in density analysis (*D*) is color-coded to show observed frequency (%). Statistical results from *E* are shown in color-coded boxes. Top row: Veh Cont vs. PTX10; middle row: Veh Cont vs. PTX20; bottom row: PTX10 vs. PTX20. $P < 0.05$ (yellow), $P < 0.01$ (orange), and $P > 0.05$ (gray). See also *SI Appendix*, Table S1 for full list of statistical results. (*F* and *G*) Quantification of nociceptive neuron morphology. (*F*) Total neurite length normalized against the area of the dendritic territory. (*G*) Neuron complexity measured by number of branch points normalized against total dendrite length. Error bars denote SEM (*E*) and SD (*F* and *G*). Mixed effect analysis with Tukey's multiple comparison posttest (*D* and *E*) and one-way ANOVA with Tukey's multiple comparison posttest (*F* and *G*).

administered paclitaxel at 1, 10, and 20 μM and induced escape behavior using global heat stimulation. We observed a significant decrease in nocifensive responses at 10 and 20 μM, but not at 1 μM (Fig. 3*A*). To determine if paclitaxel exerted an effect primarily on sensory neurons or downstream of primary nociceptors, we manipulated the downstream circuitry (*SI Appendix*, Fig. S4). We fed larvae paclitaxel and activated downstream circuitry by expressing TrpA in Down and Back (DnB) interneurons, one of the main downstream targets of larval nociceptive neurons (21). Thermogenetic activation of DnB neurons elicits bending and rolling behavior (21), so we predicted that direct activation of DnB neurons would still be able to induce rolling behavior if the nociceptive neurons were the major target of paclitaxel. Indeed, activation of DnB neurons effectively induced nociceptive behaviors with and without paclitaxel feeding. Our results are consistent with paclitaxel disrupting nociceptive behavior through action primarily on sensory neurons; however, we cannot eliminate the possibility that our thermogenetic activation approach may overcome disruptions to the interneurons.

We next examined whether integrin overexpression in nociceptive neurons can restore nocifensive behavior in paclitaxel-treated larvae. Without paclitaxel administration, we found that changes in the levels of integrins or overexpression of N-cadherin did not strongly alter nociceptive responses relative to genotype controls (*SI Appendix*, Fig. S5) (integrin down-regulation $P = 0.099$; integrin overexpression $P = 0.676$; Ncad overexpression $P = 0.971$). We found some evidence for a dose-dependent relationship between integrin levels and nocifensive responses, insofar as integrin knockdown vs. overexpression led to differences in the number of rolls initiated per nocifensive bout ($P = 0.013$). This effect on nociceptive responses could conceivably be due to functional effects arising from changes in the 3D positioning of arbors relative to the epidermis, as has been described in a prior study (41). At both 10 and 20 μM of paclitaxel, overexpression of integrins in nociceptors led to a stronger rolling response to noxious heat compared to genotype controls (Fig. 3*B*). These results together suggest that integrin overexpression in nociceptive neurons prevents functional disruption in detecting noxious heat stimuli.

Effects of Paclitaxel on Endosomal-Lysosomal Pathways and Integrin Trafficking in *Drosophila*. We next investigated the cellular changes in neurons caused by paclitaxel treatment that could be offset by augmenting integrin levels. Conceivably, these changes could include reduction in de novo integrin synthesis, reduced integrin

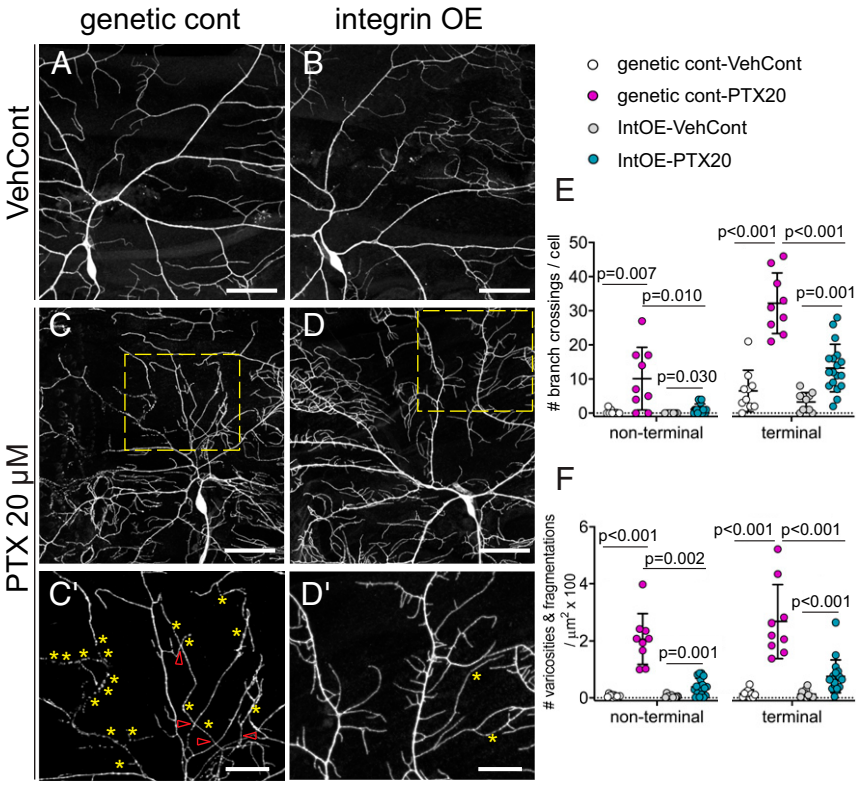

Fig. 2. Cell-specific integrin overexpression prevents paclitaxel-induced morphological changes in nociceptive neurons in *Drosophila*. All animals harbor a nociceptive neuron driver and a marker (*ppk1.9Gal4*, *ppkcd4tdgfp*) without *UAS* (indicated as genetic control) or *UAS-αPS1* and *UAS-βPS* (indicated as integrin overexpressing). (*A–D′*) Confocal micrographs of nociceptive neurons from genetic control (genetic cont, *A*, *C*, and *C′*) and integrin overexpressing (IntOE *B*, *D*, and *D′*) animals treated with vehicle (VehCont) or paclitaxel (PTX, at 20 μM). (*C′* and *D′*) Enlarged images of areas in *C* and *D* (yellow boxes) showing varicosities (yellow asterisks) and branch crossings (red arrowheads). Data were collected from three to five independent experiments (*n*): genetic cont-VehCont $n = 4$ (10 animals), genetic cont-PTX20 $n = 3$ (9 animals), integrin overexpressing (IntOE)-VehCont $n = 4$ (8 animals), IntOE-PTX20 $n = 5$ (15 animals). (Scale bars, 50 μm in *A–D* and 20 μm in *C′* and *D′*). (*E* and *F*) Quantification of paclitaxel-induced phenotypes, branch crossing and degeneration (varicosities and fragmentation), in nonterminal and terminal dendrites. Each data point represents a single cell from one larva (*SI Appendix, SI Materials and Methods*). All error bars represent SD. Kolmogorov–Smirnov test (*E*, nonterminal; *F*, terminal), one-way ANOVA with Tukey's multiple comparison posttest (*E*, terminal), and Brown–Forsythe and Welch's ANOVA with Dunnett's T3 multiple comparison posttest (*F*, nonterminal). See also *SI Appendix*, Table S1 for full list of statistical results.

recycling, and increased integrin degradation. We therefore investigated potential changes caused by paclitaxel in endosomal and lysosomal pathways in nociceptive neurons in *Drosophila*. To assess overall changes in the endocytic pathway, we chose two markers that label distinct populations of endo-lysosomal vesicles, the small GTPase Rab4 and the transporter protein Spinster (Spin) (42, 43). Rab4 mediates the early endosome to recycling endosome transition and is found in both early and recycling endosomes (43, 44). Spin plays a critical role in the autophagy-lysosome transition and is found in late endosomes, lysosomes, and autophagosomes (42, 45).

We expressed Rab4-RFP and Spin-RFP in nociceptive neurons and monitored their dynamics in primary neurites in late third-instar larvae. High-resolution time-lapse imaging (*SI Appendix, SI Materials and Methods*) revealed bidirectional trafficking of $Rab4^+$ and $Spin^+$ endosomes of various sizes and speeds (Fig. 4 *A* and *B'*). We found that effects on Rab4 and Spin trafficking were evident with both 10 and 20 μM chronic paclitaxel treatment (Fig. 4 *C–I*), indicating changes in both recycling and lysosomal pathways. Chronic paclitaxel treatment caused a higher portion of $Rab4^+$ vesicles to become stationary at the expense of both anterograde and retrograde motility (Fig. 4 *C, C'*, and *E*), with the motile pool of $Rab4^+$ vesicles showing a reduced velocity and a higher frequency of direction switching (Fig. 4 *F* and *G*). Motile vesicles showed a significant reduction in density, whereas paclitaxel treatment modestly reduced the density of stationary vesicles (Fig. 4*H*) (VehCont vs. PTX10: $P = 0.291$ and VehCont vs. PTX20: $P = 0.200$). In addition, both 10 and 20 μM paclitaxel caused a marked enlargement of some nonmotile $Spin^+$ vesicles (Fig. 4 *D*, *D'*, and *I*). Together, our results suggest disruptions in both recycling and lysosomal pathways by paclitaxel.

We next tested whether changes to the endosomal-lysosomal pathway could affect trafficking of integrins following chronic paclitaxel treatment. To examine whether the intracellular localization of integrins is changed by paclitaxel administration, we expressed YFP-Rab4, and coexpressed the α- and β-integrin subunits, αPS1 and βPS, in nociceptive neurons (Fig. 4*J*). We labeled YFP-Rab4 and βPS integrins, and used superresolution microscopy (46) to quantify their colocalization in soma, dendrites, and proximal axon. Soma volume was comparable between control and paclitaxel-treated cells (Fig. 4*K*). Rab4 density showed a modest decrease ($P = 0.062$), whereas the number of Rab4 vesicles that colocalized with integrins showed a stronger decrease upon paclitaxel treatment, particularly in dendrites (Fig. 4 *L–P*). These results suggest that paclitaxel disrupts trafficking of Rab4-mediated recycling endosomes carrying integrins in nociceptive arbors. We cannot exclude the possibility that changes in levels of protein synthesis or degradation contribute to these observations. However, our results suggest that these intracellular changes could affect the amount of integrins available on the surface to support nociceptive arbor maintenance.

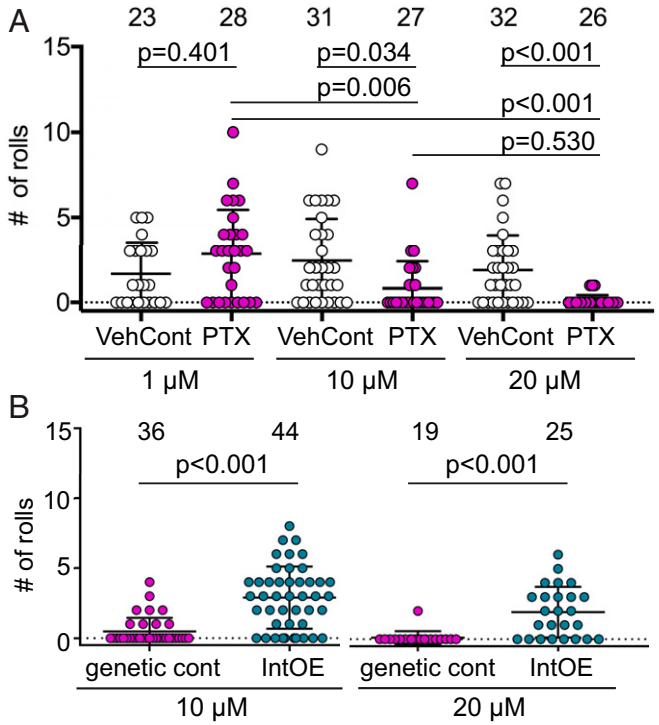

Fig. 3. Cell-specific integrin overexpression prevents paclitaxel-induced functional changes in nocifensive behavior in *Drosophila*. Quantification of nocifensive behavior evoked by global heat (40 °C). Quantification of number of rolls within 30 s upon providing a thermal stimulus to the larva in larvae fed vehicle alone (VehCont, w^{1118} genotype) (*A*), genetic control (genetic cont, lacking *UAS*), and nociceptive neuron specific integrin overexpressing (IntOE) larvae (*B*). Each data point represents a single larva. Data were collected from six (*A*) and seven (*B*) independent experiments, respectively. All error bars denote SD. Kolmogorov–Smirnov test.

Endosomal Changes Precede Early Morphological Hallmarks of Degeneration. Next, we examined whether changes in intracellular trafficking precede or follow morphological degeneration of nociceptive terminals. Instead of chronically treating larvae with paclitaxel (Fig. 4), we administered paclitaxel at 20 μM for either 48 h or 72 h and quantified changes in morphology (Fig. 5 *A–D* and *SI Appendix*, Figs. S6 and S7). For Rab4, 72-h, but not 48-h, administration of paclitaxel frequently induced varicosities in higher-order branches, but only rarely induced severe degeneration in either genetic control or Rab4-expressing nociceptive neurons (Fig. 5 *B–D* and *SI Appendix*, Figs. S6 and S7). Thus, we consider 48 h as a stage prior to paclitaxel-induced emergence of morphological degeneration and studied paclitaxel effects on Rab4 trafficking at this time point. In contrast, Spin-expressing neurons showed degeneration phenotypes in vehicle control (Fig. 5 *B* and *D* compared to *SI Appendix*, Fig. S8 *A* and *B*) and showed a modest increase in both degeneration and branch crossing phenotypes (*SI Appendix*, Fig. S8) at 48 h. Due to disruptions caused by Spin alone, we were not able to dissociate degeneration and trafficking defects and compared effects of paclitaxel to baseline degeneration phenotypes at 48 h.

To investigate potential changes preceding morphological degeneration caused by paclitaxel, we monitored the trafficking of Rab4 and Spin in primary neurites treated with paclitaxel for 48 h. Acute changes in Rab4 and Spin were similar to the phenotypes observed in animals chronically treated with paclitaxel (Figs. 4 and 5 and *SI Appendix*, Fig. S9). We found that the total number of Rab4 puncta was reduced upon paclitaxel administration and a higher portion of $Rab4^+$ vesicles became stationary (Fig. 5 *E–G*). For Spin, paclitaxel caused a significant enlargement of $Spin^+$ vesicles by 48 h (*SI Appendix*, Fig. S9 *D* and *F*).

Overexpression of integrins affected these vesicles differently following 48-h paclitaxel administration. Cooverexpression of integrins with Rab4 prevented paclitaxel-induced changes in Rab4 (*SI Appendix*, Fig. S9 *A–C*), whereas coexpression of integrins and Spin did not rescue the enlargement phenotype (*SI Appendix*, Fig. S9 *E* and *F*). Together, our results suggest that paclitaxel-induced intracellular trafficking changes precede morphological degeneration rather than emerge as by-products of the morphological changes caused by chronic paclitaxel administration. Furthermore, integrins appear to impact trafficking of $Rab4^+$ vesicles, providing a possible mechanism of integrin-mediated protection in a CIPN model.

ITGB1 Transduction in Adult Mouse DRG Neurons Prevents Axon Degeneration. We next asked whether effects on endosomal-lysosomal pathways and integrin-mediated protection from paclitaxel are also observed in vertebrate neurons. First, we examined the effect of paclitaxel treatment on Rab4 endosomes and Lamp1 lysosomes. Consistent with our findings in *Drosophila*, we found that the motility of $Rab4^+$ and $Lamp1^+$ vesicles is altered prior to morphological degeneration of mouse DRG neurons (*SI Appendix*, Figs. S10 and S11). We next asked whether integrin-mediated protection from paclitaxel is also observed in mouse DRG neurons. Since augmentation of a single integrin subunit can recruit endogenous subunit partners (47, 48), we chose to transduce the human integrin β1 subunit 1 (ITGB1), a major β-subunit in integrin heteromeric dimers in adult rodent DRG neurons (49–51). Lentivirus-mediated delivery of ITGB1 was carried out in adult DRG neurons at 5 d in vitro (DIV) prior to treatment with either vehicle or 50 nM paclitaxel for 72 h starting at 12 DIV, an experimental paradigm that had been previously shown to induce early signs of axon degeneration and reduce axon growth (8). To better capture the changes in the cells in culture and to avoid selection bias, we sampled large areas (2×2 mm^2) for quantification. We found that treating DRG neurons with paclitaxel resulted in axon loss and axon fragmentation (Fig. 6 *A* and *B'*), as shown by a significant decrease in total axon area and an increased degeneration index (the ratio between fragmented axon and total axon areas) compared to control DRG neurons (Fig. 6 *E* and *F* and *SI Appendix*, Fig. S12). Consistent with the protective capacity observed in *Drosophila* nociceptive neurons, DRG neurons transduced with ITGB1 prior to paclitaxel treatment showed no change in total axon area and a reduced degeneration index compared to paclitaxel-treated control neurons (Fig. 6 *E* and *F*).

To examine whether integrin membrane trafficking is affected by paclitaxel treatment in DRG neurons, we next performed a surface biotinylation assay to measure total and surface levels of ITGB1. Cell lysates were collected after 24, 48, and 72 h following either vehicle or 50 nM paclitaxel treatment starting at 12 DIV. We found that treating DRG neurons with paclitaxel did not change total levels of ITGB1 arguing against an effect of paclitaxel on integrin de novo synthesis or turnover, but caused a significant reduction of ITGB1 localization at the cell surface at all observed time points in vitro (Fig. 6 *G–I*). These results suggest a conserved protective role for integrins in *Drosophila* and vertebrate CIPN models.

Discussion

In this study, we used *Drosophila* larval sensory neurons and adult mouse DRG neurons in culture to investigate the mechanisms of sensory neuropathy induced by paclitaxel. We analyzed the morphological changes induced by paclitaxel in sensory neurons, and report quantitative changes in branch pattern arising from paclitaxel exposure. Cellular, genetic, biochemical, and behavioral approaches suggest that integrin trafficking via the endosomal-lysosomal pathway is disrupted in sensory neurons treated with

NEUROSCIENCE

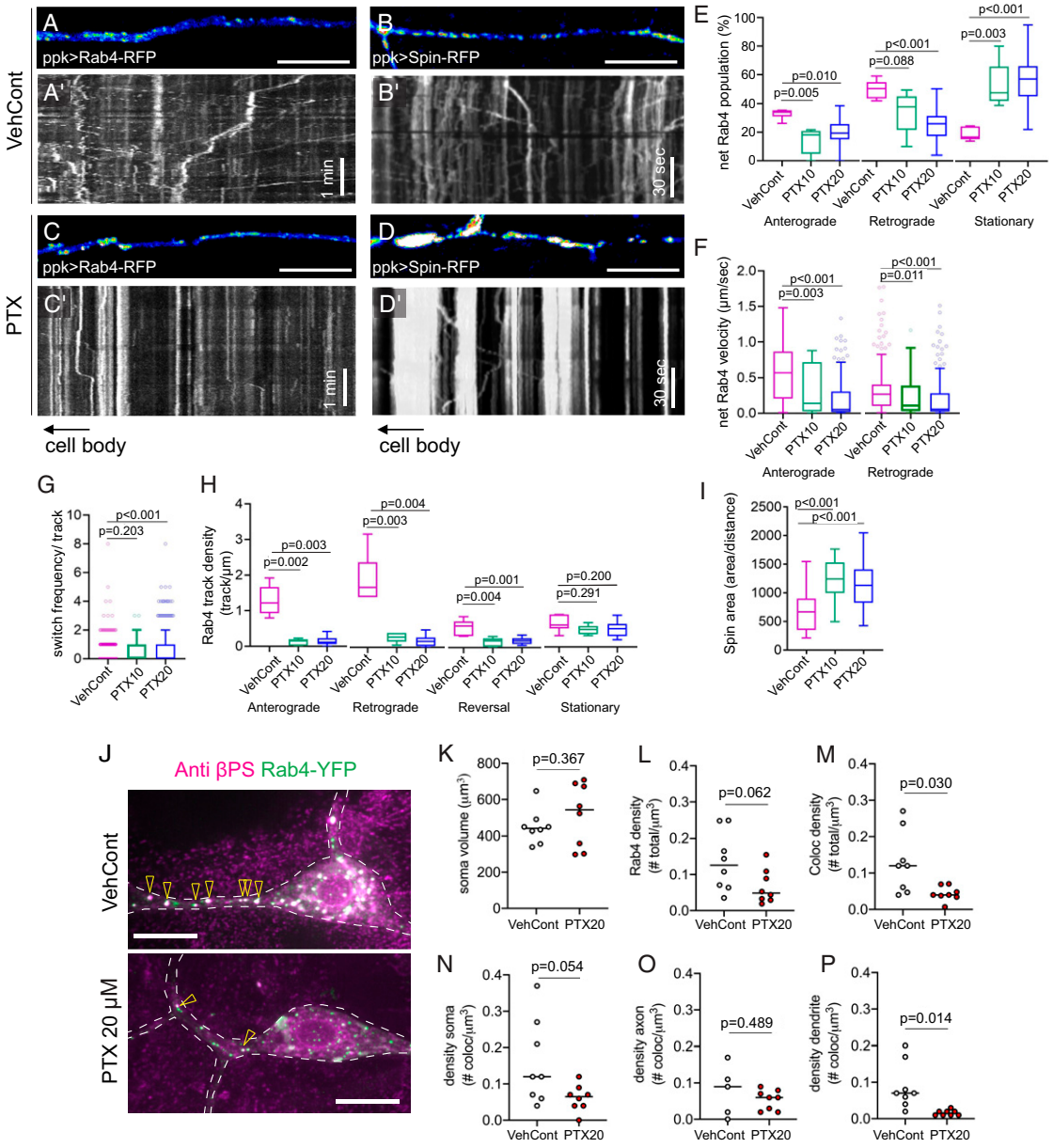

Fig. 4. Paclitaxel affects endosomal-lysosomal pathways and changes integrin trafficking in *Drosophila*. (*A–D′*) Rab4-mRFP (*A*, *A′*, *C*, and *C′*) and Spin-myc-mRFP (*B*, *B′*, *D*, and *D′*) were expressed in nociceptive neurons using *ppk1.9-Gal4*. Rab4-RFP or Spin-RFP are shown in nociceptor peripheral dendrites in still images. Movements are visualized by kymographs in animals treated with vehicle (VehCont) and paclitaxel (PTX). For paclitaxel-treated neurons, 10- and 20-µM treatment resulted in qualitatively similar kymographs and only 20-µM–treated neurons are shown. Data were collected from two to four independent experiments (*n*): Rab4-VehCont $n = 2$ (three animals), Rab4-PTX10 $n = 2$ (two animals), Rab4-PTX20 $n = 2$ (six animals), Spin-VehCont $n = 4$ (nine animals), Spin-PTX10 $n = 2$ (seven animals), and Spin-PTX20 $n = 2$ (three animals). (Scale bars, 10 µm.) (*E–H*) Quantification of net Rab4 vesicle population showing anterograde, retrograde, and stationary vesicles (*E*, VehCont $n = 6$, PTX10 $n = 5$, PTX20 $n = 27$, *n* denotes the number of individual kymographs), net velocity (*F*, VehCont $n = 247$, PTX10 $n = 26$, PTX20 $n = 167$, *n* denotes the number of individual tracks), switch frequency (*G*, VehCont $n = 639$, PTX10 $n = 91$, PTX20 $n = 418$, *n* denotes the number of individual tracks), and track density (*H*, VehCont $n = 6$, PTX10 $n = 5$, PTX20 $n = 27$, *n* denotes the number of individual kymographs). (*I*) Quantification of Spin vesicle population occupancy in dendrites. An area corresponding to 20 frames with minimal animal movement was selected from each kymograph. Fluorescent area under the curve was measured and normalized to distance selected for imaging. Each data point represents a kymograph collected from live imaging (VehCont $n = 21$, PTX10 $n = 25$, PTX20 $n = 14$, *n* denotes for the number of individual kymographs). (*J–P*) YFP-Rab4 and integrins were coexpressed in nociceptive neurons by using the nociceptive neuron driver *ppk1.9-Gal4* in animals treated with vehicle and paclitaxel (20 µM). Soma, axon, and sensory dendrites were segmented for quantification. Data were collected from three independent experiments from vehicle and paclitaxel-treated groups, respectively. Micrographs collected by using superresolution iSIM microscopy, visualizing integrin βsubunit (βPS) by antibody labeling (endogenous + overexpressed; magenta) and Rab4 by antibody labeling against GFP (overexpressed only; green), and maximum intensity *z*-projection images are shown. Arrowheads denote colocalized puncta between integrin βPS and Rab4 (labeled white). (*K–M*) Soma volume (*K*), normalized density (per volume) of Rab4 puncta (*L*), colocalized puncta between integrin βPS and Rab4 in all segments combined (*M*). (*N–P*) Normalized density (per volume) of colocalized puncta between integrin βPS and Rab4 in soma (*N*), axon (*O*), and dendrite (*P*). Each data point refers to a single cell used for quantification. (Scale bars, 10 µm.) (*E–I*) Data were plotted using Tukey's box and whiskers. Kolmogorov–Smirnov test, one-way ANOVA with Tukey's multiple comparison posttest, or Brown–Forsythe and Welch's ANOVA with Dunnett's T3 multiple comparison posttest. (*K–P*) Lines refer to median. Kolmogorov–Smirnov test or Welch's *t* test. See also *SI Appendix*, Table S1 for full description of statistical results.

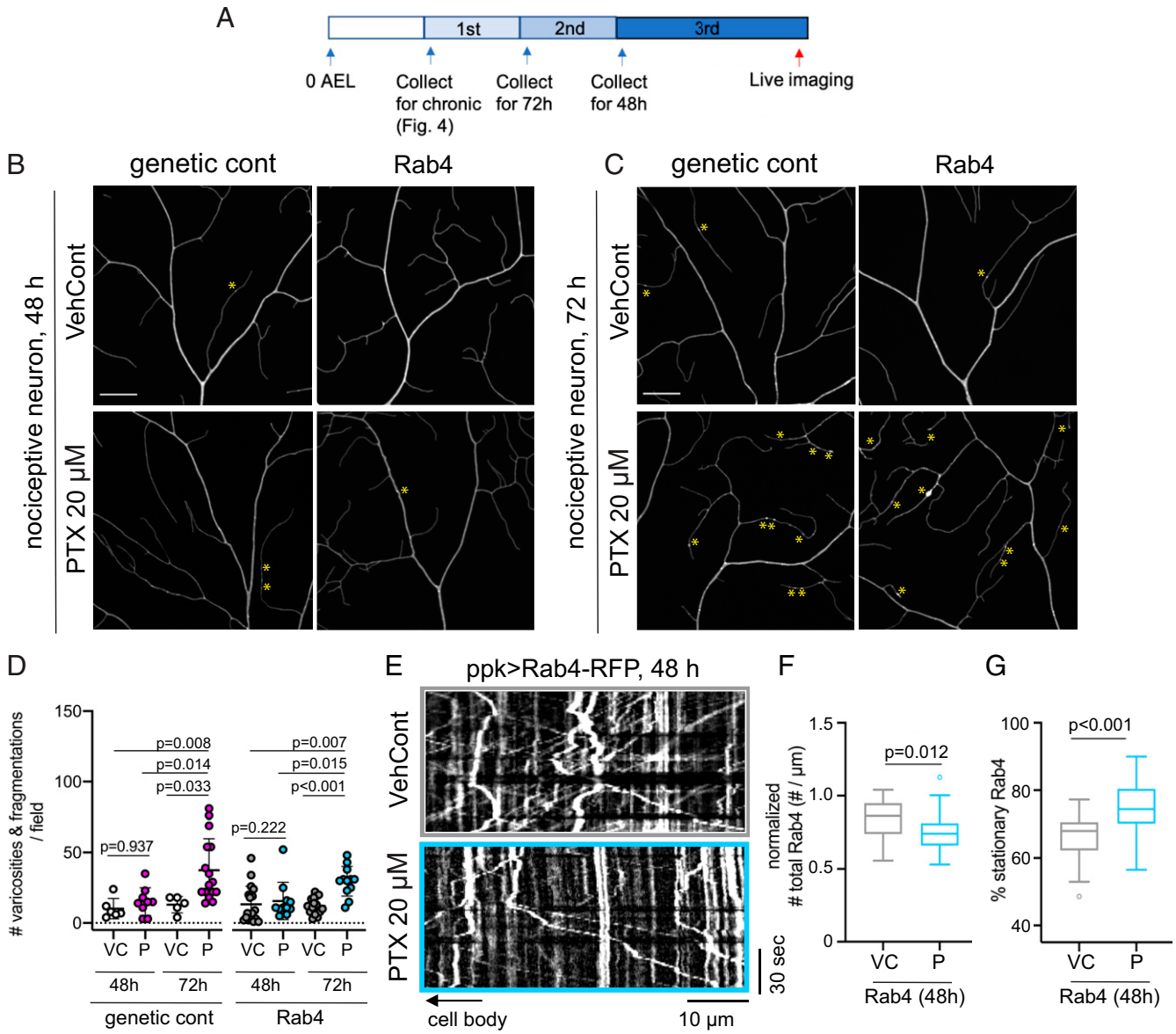

Fig. 5. Paclitaxel-induced endosomal changes precede early morphological hallmarks of degeneration in *Drosophila*. (*A*) Timeline of paclitaxel treatments and live imaging. (*B–D*) Examples of micrographs and quantification of the integrity of nociceptive dendrites after paclitaxel treatments for 48 h (*B*) and 72 h (*C*). All animals harbor a nociceptive neuron driver and a marker (*ppk1.9Gal4*, *ppkcd4tdgfp*) without *UAS* (genetic cont) or *UAS-Rab4-mRFP* (Rab4). (Scale bars, 20 μm.) Scale bars in the first panels of *B* and *C* apply to all subsequent panels. Yellow asterisks indicate varicosities and fragmentation. (*D*) Degeneration was quantified using images collected from live animals. VC: vehicle control; P: 20 μM paclitaxel. Data were collected from genetic cont VC 48 h $n = 2$ (4 animals), genetic cont-VC 72 h $n = 2$ (3 animals), genetic cont-P 48 h $n = 2$ (4 animals), genetic cont-P 72 h $n = 2$ (5 animals), Rab4-VC 48 h $n = 4$ (10 animals), Rab4-VC 72 h $n = 2$ (7 animals), Rab4-P 48 h $n = 2$ (5 animals), and Rab4-P 72 h $n = 2$ (4 animals). Each data point represents a quantification of a single cell, two to three cells collected from each animal. Error bars = SD. One-way ANOVA with Tukey's multiple comparisons posttest. (*E*) Rab4-mRFP expressing nociceptive neurons imaged after 48 h of 20 μM paclitaxel feeding. Movements are visualized by kymographs in animals treated with vehicle (VC) and paclitaxel (P). All larvae were fed paclitaxel or vehicle for 48 h starting from the early third-instar stage. (*F* and *G*) Quantification of Rab4 vesicles. The number of total Rab4 vesicles is reduced and the portion of stationary Rab4 increased in paclitaxel treated cells. Number of individual kymographs used: Rab4-VC $n = 22$, Rab4-P $n = 50$; one to four kymographs were generated from each cell. Data were collected from Rab4-VC 48 h $n = 4$ (10 animals) and Rab4-P 48 h $n = 2$ (5 animals). Field size is 243 × 243 μm^2, a full field of view using a 40× objective, including the center of a single cell.(*F* and *G*) All data were plotted using Tukey's box and whiskers. Unpaired *t* test.

paclitaxel, and that integrin overexpression counteracts the propensity of paclitaxel to disrupt sensory neuron maintenance. These main findings were seen in both fly and vertebrate neurons. In addition, we used DRG neurons to show that surface availability of integrins is reduced by paclitaxel. We propose that one primary neuropathic effect of paclitaxel in sensory neurons is to impact the delivery of key cell adhesion receptors involved in interactions with the extracellular environment by disrupting recycling pathways. This disruption could lead to deficits in arbor maintenance, and eventually degeneration of sensory terminals.

Integrins Provide a Link between Sensory Neurons and the Extracellular Environment. Because of their small caliber and location adjacent to a highly dynamic epidermis, IENFs are highly sensitive peripheral sensory structures (9). Our data show that integrin trafficking is impacted by paclitaxel and that augmenting integrin

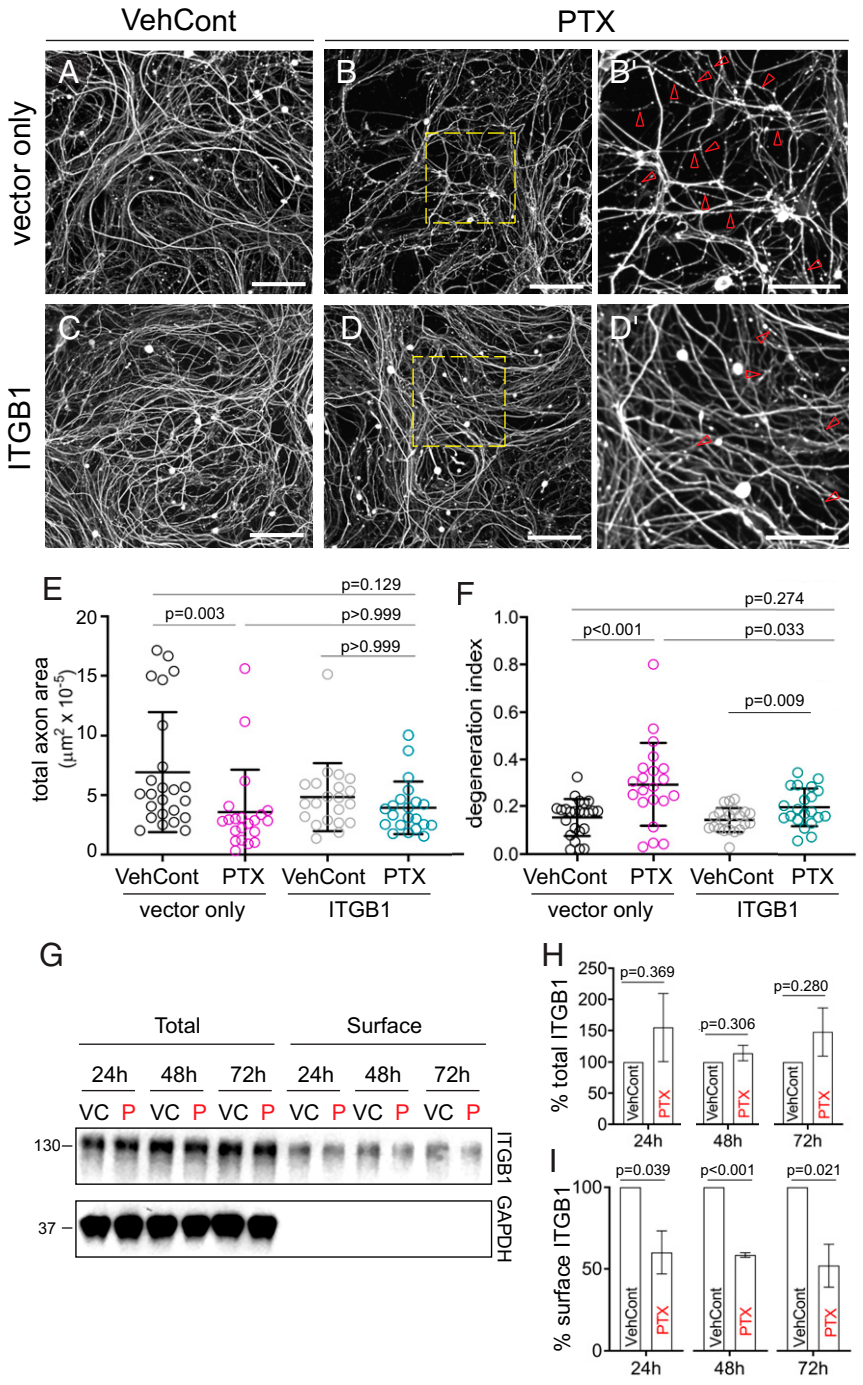

Fig. 6. ITGB1 overexpression prevents paclitaxel-induced degeneration in adult mouse DRG neurons in vitro. (*A–D′*) Micrographs of DRG neurons treated with control virus and vehicle (*A*), control virus and paclitaxel (*B*), ITGB1 virus and vehicle (*C*), and ITGB1 virus and paclitaxel (*D*). (*B′* and *D′*). Enlarged images of areas indicated by yellow boxes in *B* and *D* showing fragmentation (red arrowheads). Axons are labeled with NF200, which labeled axons of all subpopulation of DRG neurons in vitro. Data were collected from four independent experiments. (Scale bars, 200 μm in *A–D* and 100 μm *B′* and *D′*.) (*E* and *F*) Quantification of total area of axon (*E*) and axon degeneration (*F*) using a degeneration index measurement (degenerated area/total area of NF200 positive signal), calculated across the entire image. Two nonoverlapping areas (2×2 mm^2) were randomly selected from each well, and each data point refers to each region of interest. (*G–I*) Detection and quantification of total and surface levels of ITGB1 in DRG neurons after paclitaxel treatment. A representative blot is shown from three independent experiments. DRG neurons were treated with vehicle control (VC) and paclitaxel (P) and collected for surface biotinylation labeling after 24, 48, and 72 h. Percent of ITGB1 surface expression at each time point is quantified for comparison. Data were collected from three independent experiments. Error bars denote SD (*E* and *F*) or SEM (*H* and *I*). Kruskal–Wallis test with Dunn's multiple comparison posttest (*E*), Kolmogorov–Smirnov test or Welch's *t* test (*F*) and unpaired *t* tests (*H* and *I*). See also *SI Appendix*, Table S1 for a full list of statistical results.

levels may help to restore neuronal interactions with the extracellular environment. A valuable next step would be assessing the effect of integrin augmentation in preclinical models in vivo. Given the accessibility of the peripheral environment, identification of the ligands that are involved in this protection is an important goal for future studies. Alternative signaling pathways could also contribute to integrin-mediated protection. For example, during the development of larval nociceptive neurons integrins colocalize with the conserved receptor tyrosine kinase Ret that is required for regular patterning, dynamic growth, and adhesion of dendritic branches (52, 53). Since adhesive roles for Ret and integrins are conserved in vertebrates (54), it is possible that similar receptors and ligands may interact with integrins to mediate interactions between IENFs and their extracellular environment.

There are important distinctions between *Drosophila* sensory dendrites and DRG axons, and indeed, we report distinct and shared phenotypes for these processes upon treatment with paclitaxel. We propose that the ability of integrins to counter degeneration in both systems is consistent with roles in both axons and dendrites, and our findings argue for some generality in these two models. Similarities could conceivably arise because peripheral sensory terminals share anatomical features such as naked endings and a close relationship with a substrate comprised of ECM. These features could render thin terminal sensory processes more susceptible to toxins that disrupt the connection to the ECM. The peculiarities of each system, as well as the in vivo vs. in vitro execution of the experiments, likely underlie the distinct paclitaxel-induced phenotypes we observed, such as branching and self-avoidance in vivo in sensory dendrites. As with their role in da neuron dendrites, integrins may play a critical role in maintaining the peripheral processes of mature sensory neurons. Supporting this hypothesis, the localization of tagged virally expressed or endogenous integrins is limited to the somatodendritic compartment in the mature CNS neurons, whereas integrins also traffic to axons of adult DRG sensory neurons and retinal ganglion cells (55–59).

Evidence that Endocytic Changes Caused by Paclitaxel Perturb Integrin Recycling. Paclitaxel is a microtubule binding agent and interferes with dynamic instability of microtubules required for mitosis in cell division, leading to apoptosis of cancer cells (60). However, we currently have a limited understanding of how paclitaxel-induced changes disrupt intracellular transport in neurons and whether such disruption contributes to peripheral neuropathy (8, 61–65). Different studies consistently report that paclitaxel treatment results in changes to intracellular transport—including mitochondria, microtubule motor proteins, and lysosomes—but there is no strong consensus on the extent to which such changes contribute to peripheral sensory neuropathy. Prior studies also indicate that paclitaxel disrupts trafficking of specific intracellular cargos from the nucleus, including RNA granules required for maintenance of sensory terminals and nuclear encoded mRNA required for mitochondrial function (26, 66).

In our present study, we provide evidence that paclitaxel disrupts trafficking of recycling endosomes in *Drosophila* peripheral nociceptive arbors and adult mouse neurons in vitro. Specifically, we found a decrease in small GTPase Rab4 motility in both *Drosophila* and mouse, which precedes morphological degeneration in both systems. We also report a decrease in integrin colocalization with Rab4 vesicles in *Drosophila* sensory arbors in vivo after chronic paclitaxel treatment. Rab4 acts at the interface between early/sorting endosomes and recycling endosomes, and is a key mediator of integrin recycling (30, 67, 68). Perturbation of Rab4 motility and availability would likely lead to reduced integrin recycling, as further corroborated by our results indicating a reduction of ITGB1 surface expression levels in DRG neurons in vitro. Reciprocally, we found that integrin augmentation prevents paclitaxel-induced Rab4 changes in *Drosophila* following acute treatment, suggesting an intracellular mechanism of integrin-mediated protection that may ameliorate pathological progress by influencing vesicular trafficking. Given the disruption of integrin delivery to the cell surface in DRG neurons, augmentation of integrins may increase the probability that integrins reside in the membrane, facilitating the maintenance of the neuron–ECM link. Additionally, our data suggest that increased integrins in endosomes may affect their trafficking or downstream signaling events, ultimately changing integrin delivery and function (69). Using two complementary models, our study supports a conserved mechanism of pathology and protection by integrins. Strikingly, in both *Drosophila* larval sensory neurons and adult DRG neurons, paclitaxel treatment leads to disruption of integrin membrane trafficking, and augmentation of integrins was sufficient to protect sensory neurons from paclitaxel. In addition to other studies showing selective intracellular trafficking changes (26, 66), our results support a contribution of distinct endocytic changes to paclitaxel toxicity.

We also found enlargement of $Spin^{+}$ vesicles in larval nociceptive neurons upon paclitaxel treatment. The significance of lysosome enlargement to neuropathic changes is not currently known, and our results indicate that they are unlikely to be directly linked with integrin pathways. Prior studies have linked perturbation of lysosomal degradation, lysosome enlargement, and progressive neurodegeneration (45, 70–74). Several mechanisms could explain the lysosome enlargement phenotype, including defects in lysosomal degradation machinery (72), failure in autophagic lysosome reformation (45, 70), and defective endosomal-to-lysosomal transport (71, 73, 74). Furthermore, while a prior study showed that paclitaxel-induced neurotoxicity is independent of lysosome trafficking in a mouse CIPN model in vitro (8), we found a decreased lysosome motility in DRG neurons starting from 24-h paclitaxel treatment, a time point prior to morphological degeneration of DRG axons. This difference may reflect the timeline of emergence of toxicity, different scoring methods, or dose-dependent toxicity of paclitaxel: 25 nM (8) vs. 50 nM (present study). Our current study does not prove causality between lysosomal changes and degeneration; however, it suggests that lysosomal changes might be a hallmark of CIPN pathology. Thus, examination of whether paclitaxel impacts integrin recycling by affecting lysosomal activity in chronic neuropathic conditions will be an important goal for future studies.

A number of survival and maintenance factors are modulated upon paclitaxel treatment. Paclitaxel reduces axonal localization of the prosurvival factor Bclw, but not Bcl2 or Bclx, in embryonic sensory neuron culture (26). MMP13 was selectively activated in epidermal cells but not in neurons upon paclitaxel treatment (25). Similarly, integrins may be one of several cargos that are reduced in the plasma membrane as a consequence of paclitaxel-induced disruption in endo-lysosomal compartments. Integrin-mediated pathways may be highly susceptible to these changes because integrin surface abundance relies heavily on recycling and integrins may be continuously required in dynamic cellular compartments, such as nociceptive terminals or the leading edge of cancer cells (19, 20, 67, 68, 75). Surface proteomic analysis may address the broader impact of paclitaxel on the levels of membrane proteins required for maintenance of sensory neurons. Our study provides motivation for further studies of membrane proteins in CIPN.

Neuronal Substrate Interactions in CIPN. IENF density correlates with the severity of sensory peripheral neuropathy in patients, and the change in morphology serves as a strong predictor of symptoms and prognosis in clinics (2, 11, 12, 76–80). In patients with chronic peripheral neuropathy, axon terminals are present in the subepidermal layer but absent in the epidermis (77). It is therefore critical to understand the factors that help maintain terminal nerve fibers and that could prevent their degeneration in CIPN. Our results show that integrin supplementation promotes the maintenance of

sensory terminals upon paclitaxel treatment in *Drosophila* and in DRG neurons cultured in vitro, suggesting that integrins could be a key factor in somatosensory terminal maintenance to counteract CIPN. It will be essential to know whether these effects translate to vertebrate axons in vivo targeting the epidermis. Notably, other studies have shown that integrin levels can increase after neuron injury, and levels correlate with regenerative ability (81). Differences in integrin levels between peripheral DRG neurons and neurons in the CNS may correlate with different abilities of these neurons to regenerate (55). Together, the present study and previous results suggest that integrins could be major determinants of neuronal maintenance in different types of injuries in the nervous system.

Currently, there is no effective method of preventing or treating CIPN other than stopping chemotherapeutic treatment or changing the chemotherapy regimen. Up to 80% of CIPN patients treated with paclitaxel still report symptoms in the long term after the cessation of chemotherapeutic treatment (22, 23). Limited symptomatic relief is provided by opioid analgesics, antidepressants, or anticonvulsants (23, 82). The in vivo *Drosophila* model to study chemotherapeutic-induced changes in neurons has led to the identification of integrins as a protective pathway effective also in vertebrate sensory neurons in vitro. Accumulating evidence underscores the importance of intrinsic mechanisms in preventing neural degeneration, yet the efficacy of these approaches in relevant in vivo contexts is poorly understood. The present study provides evidence that changes in the ability of neurons to link to, and interact with, the extracellular environment results in neuropathic changes in multiple models. Further studies of substrate interactions in these models might provide important insights into the mechanisms, etiology, and treatment of CIPN.

Materials and Methods

Further details of materials and methods can be found in *SI Appendix, SI Materials and Methods*.

Larval Assay Set-up for Paclitaxel Treatment. Paclitaxel (Tocris Bioscience) was diluted to 5 mM in ethanol, and fresh aliquots of paclitaxel were diluted to a final concentration of 1, 10, 20, or 30 μM in 1× PBS. A matching concentration of ethanol was added as a vehicle control. This solution was used to make food using instant *Drosophila* medium (Formula 4-24, Carolina Biological Supply Company) immediately before starting the larval assay. Embryos were collected on grape plates with yeast paste made with 0.5% propionic acid for chronic treatment and second instar or early third-instar larvae were collected manually (Fig. 5*A*) directly from standard molasses *Drosophila* media for acute treatment.

Global Activation Heat Nocifensive Assay and Behavioral Analysis. Global activation heat nocifensive assays were performed as previously described (21). The number of 360° rolls was scored by using trachea as a reference for the dorsal region of the larva.

Adult Mouse DRG Culture and Paclitaxel Treatment. All protocols and procedures used in this study to prepare primary culture of DRG neurons were approved by the Institutional Animal Care and Use Committee at Columbia University and according to the *Guide for the Care and Use of Laboratory Animals* distributed by the National Institutes of Health (83). DRG from 8- to 12-wk-old C57BL/6J mice of both sexes were dissected, dissociated, and plated in a 12-well plate. Paclitaxel was treated starting on 12 DIV at a final concentration of 50 nM; 1 μL of DMSO was added as a vehicle control.

Data Availability. All other study data are included in the article and supporting information.

ACKNOWLEDGMENTS. We thank the Thompson Family Foundation Initiative (TFFI) at Columbia University for funding and members of TFFI for feedback and helpful discussions; W.B.G. laboratory and F.B. laboratory members for helpful discussions and feedback; Clotilde Huet-Calderwood and David Calderwood (Yale University) for providing ITGB1 plasmids; Siqian Feng, Susumu Antoku, and Xiaoyi Qu for cloning advice; Daniel Iascone for help with using the Vaa3D plugin; Terry Hafer for help with live imaging preparation for larvae; Tommy Kahn and Robert Cudmore (The Johns Hopkins University) for Python codes for blinding files; and the Zuckerman Institute's Cellular Imaging platform for instrument use and technical advice. This work was funded by TFFI awards (to W.B.G., to W.B.G. and F.B., and to F.B.); NIH/National Institute on Aging R01AG050658 (to F.B.); NIH/National Institute of Neurological Disorders and Stroke R21NS120076 (to F.B.); Italian Ministry of Education, University and Research PRIN-2017FJC3-004 (to M.E.P.); and NIH F31NS098765 (to S.E.G.).

1. M. Seretny *et al.*, Incidence, prevalence, and predictors of chemotherapy-induced peripheral neuropathy: A systematic review and meta-analysis. *Pain* **155**, 2461–2470 (2014).
2. G. Cavaletti, P. Marmiroli, Chemotherapy-induced peripheral neurotoxicity. *Nat. Rev. Neurol.* **6**, 657–666 (2010).
3. K. C. Chua, D. L. Kroetz, Genetic advances uncover mechanisms of chemotherapy-induced peripheral neuropathy. *Clin. Pharmacol. Ther.* **101**, 450–452 (2017).
4. Y. Han, M. T. Smith, Pathobiology of cancer chemotherapy-induced peripheral neuropathy (CIPN). *Front. Pharmacol.* **4**, 156 (2013).
5. G. Cavaletti *et al.*; Toxic Neuropathy Consortium of the Peripheral Nerve Society, Chemotherapy-induced peripheral neurotoxicity: A multifaceted, still unsolved issue. *J. Peripher. Nerv. Syst.* **24** (suppl. 2), S6–S12 (2019).
6. M. R. Bhattacharya *et al.*, A model of toxic neuropathy in Drosophila reveals a role for MORN4 in promoting axonal degeneration. *J. Neurosci.* **32**, 5054–5061 (2012).
7. J. M. Brazill, B. Cruz, Y. Zhu, R. G. Zhai, Nmnat mitigates sensory dysfunction in a *Drosophila* model of paclitaxel-induced peripheral neuropathy. *Dis. Model. Mech.* **11**, dmm032938 (2018).
8. E. L. Gornstein, T. L. Schwarz, Neurotoxic mechanisms of paclitaxel are local to the distal axon and independent of transport defects. *Exp. Neurol.* **288**, 153–166 (2017).
9. G. J. Bennett, G. K. Liu, W. H. Xiao, H. W. Jin, C. Siau, Terminal arbor degeneration—A novel lesion produced by the antineoplastic agent paclitaxel. *Eur. J. Neurosci.* **33**, 1667–1676 (2011).
10. J. Boyette-Davis, P. M. Dougherty, Protection against oxaliplatin-induced mechanical hyperalgesia and intraepidermal nerve fiber loss by minocycline. *Exp. Neurol.* **229**, 353–357 (2011).
11. G. Lauria *et al.*, Axonal swellings predict the degeneration of epidermal nerve fibers in painful neuropathies. *Neurology* **61**, 631–636 (2003).
12. R. E. Schmidt *et al.*, Dystrophic axonal swellings develop as a function of age and diabetes in human dorsal root ganglia. *J. Neuropathol. Exp. Neurol.* **56**, 1028–1043 (1997).
13. K. D. Tanner, J. D. Levine, K. S. Topp, Microtubule disorientation and axonal swelling in unmyelinated sensory axons during vincristine-induced painful neuropathy in rat. *J. Comp. Neurol.* **395**, 481–492 (1998).
14. W. H. Xiao, H. Zheng, G. J. Bennett, Characterization of oxaliplatin-induced chronic painful peripheral neuropathy in the rat and comparison with the neuropathy induced by paclitaxel. *Neuroscience* **203**, 194–206 (2012).
15. P. R. Bergstresser, J. R. Taylor, Epidermal 'turnover time'—A new examination. *Br. J. Dermatol.* **96**, 503–509 (1977).
16. W. B. Grueber, L. Y. Jan, Y. N. Jan, Tiling of the Drosophila epidermis by multidendritic sensory neurons. *Development* **129**, 2867–2878 (2002).
17. R. Y. Hwang *et al.*, Nociceptive neurons protect Drosophila larvae from parasitoid wasps. *Curr. Biol.* **17**, 2105–2116 (2007).
18. Y. Xiang *et al.*, Light-avoidance-mediating photoreceptors tile the Drosophila larval body wall. *Nature* **468**, 921–926 (2010).
19. C. Han *et al.*, Integrins regulate repulsion-mediated dendritic patterning of drosophila sensory neurons by restricting dendrites in a 2D space. *Neuron* **73**, 64–78 (2012).
20. M. E. Kim, B. R. Shrestha, R. Blazeski, C. A. Mason, W. B. Grueber, Integrins establish dendrite-substrate relationships that promote dendritic self-avoidance and patterning in Drosophila sensory neurons. *Neuron* **73**, 79–91 (2012).
21. A. Burgos *et al.*, Nociceptive interneurons control modular motor pathways to promote escape behavior in *Drosophila*. *eLife* **7**, e26016 (2018).
22. D. L. Hershman *et al.*, Association between patient reported outcomes and quantitative sensory tests for measuring long-term neurotoxicity in breast cancer survivors treated with adjuvant paclitaxel chemotherapy. *Breast Cancer Res. Treat.* **125**, 767–774 (2011).
23. A. Shah *et al.*, Incidence and disease burden of chemotherapy-induced peripheral neuropathy in a population-based cohort. *J. Neurol. Neurosurg. Psychiatry* **89**, 636–641 (2018).
24. K. M. Wozniak *et al.*, Peripheral neuropathy induced by microtubule-targeted chemotherapies: Insights into acute injury and long-term recovery. *Cancer Res.* **78**, 817–829 (2018).
25. T. S. Lisse *et al.*, Paclitaxel-induced epithelial damage and ectopic MMP-13 expression promotes neurotoxicity in zebrafish. *Proc. Natl. Acad. Sci. U.S.A.* **113**, E2189–E2198 (2016).
26. S. E. Pease-Raissi *et al.*, Paclitaxel reduces axonal Bclw to initiate IP_3R1-dependent axon degeneration. *Neuron* **96**, 373–386.e6 (2017).
27. D. B. Reichling, J. D. Levine, Pain and death: Neurodegenerative disease mechanisms in the nociceptor. *Ann. Neurol.* **69**, 13–21 (2011).
28. G. S. Marrs *et al.*, Dendritic arbors of developing retinal ganglion cells are stabilized by beta 1-integrins. *Mol. Cell. Neurosci.* **32**, 230–241 (2006).

29. E. M. Moresco, S. Donaldson, A. Williamson, A. J. Koleske, Integrin-mediated dendrite branch maintenance requires Abelson (Abl) family kinases. *J. Neurosci.* **25**, 6105–6118 (2005).
30. P. Moreno-Layseca, J. Icha, H. Hamidi, J. Ivaska, Integrin trafficking in cells and tissues. *Nat. Cell Biol.* **21**, 122–132 (2019).
31. P. P. Di Fiore, P. De Camilli, Endocytosis and signaling. An inseparable partnership. *Cell* **106**, 1–4 (2001).
32. M. von Zastrow, A. Sorkin, Signaling on the endocytic pathway. *Curr. Opin. Cell Biol.* **19**, 436–445 (2007).
33. F. B. Gao, J. E. Brenman, L. Y. Jan, Y. N. Jan, Genes regulating dendritic outgrowth, branching, and routing in Drosophila. *Genes Dev.* **13**, 2549–2561 (1999).
34. M. E. Hughes *et al*., Homophilic Dscam interactions control complex dendrite morphogenesis. *Neuron* **54**, 417–427 (2007).
35. B. J. Matthews *et al*., Dendrite self-avoidance is controlled by Dscam. *Cell* **129**, 593–604 (2007).
36. P. Soba *et al*., Drosophila sensory neurons require Dscam for dendritic self-avoidance and proper dendritic field organization. *Neuron* **54**, 403–416 (2007).
37. P. Doherty, L. H. Rowett, S. E. Moore, D. A. Mann, F. S. Walsh, Neurite outgrowth in response to transfected N-CAM and N-cadherin reveals fundamental differences in neuronal responsiveness to CAMs. *Neuron* **6**, 247–258 (1991).
38. T. A. Ferguson, S. S. Scherer, Neuronal cadherin (NCAD) increases sensory neurite formation and outgrowth on astrocytes. *Neurosci. Lett.* **522**, 108–112 (2012).
39. T. Ohyama *et al*., High-throughput analysis of stimulus-evoked behaviors in Drosophila larva reveals multiple modality-specific escape strategies. *PLoS One* **8**, e71706 (2013).
40. W. D. Tracey Jr, R. I. Wilson, G. Laurent, S. Benzer, painless, a Drosophila gene essential for nociception. *Cell* **113**, 261–273 (2003).
41. N. Jiang *et al*., A conserved morphogenetic mechanism for epidermal ensheathment of nociceptive sensory neurites. *eLife* **8**, e42455 (2019).
42. Y. Nakano *et al*., Mutations in the novel membrane protein spinster interfere with programmed cell death and cause neural degeneration in Drosophila melanogaster. *Mol. Cell. Biol.* **21**, 3775–3788 (2001).
43. B. Sönnichsen, S. De Renzis, E. Nielsen, J. Rietdorf, M. Zerial, Distinct membrane domains on endosomes in the recycling pathway visualized by multicolor imaging of Rab4, Rab5, and Rab11. *J. Cell Biol.* **149**, 901–914 (2000).
44. C. C. Hoogenraad *et al*., Neuron specific Rab4 effector GRASP-1 coordinates membrane specialization and maturation of recycling endosomes. *PLoS Biol.* **8**, e1000283 (2010).
45. Y. Rong *et al*., Spinster is required for autophagic lysosome reformation and mTOR reactivation following starvation. *Proc. Natl. Acad. Sci. U.S.A.* **108**, 7826–7831 (2011).Corrected in: *Proc. Natl. Acad. Sci. U.S.A.* **108**, 11297 (2011).
46. A. G. York *et al*., Instant super-resolution imaging in live cells and embryos via analog image processing. *Nat. Methods* **10**, 1122–1126 (2013).
47. M. L. Condic, Adult neuronal regeneration induced by transgenic integrin expression. *J. Neurosci.* **21**, 4782–4788 (2001).
48. C. Huet-Calderwood *et al*., Novel ecto-tagged integrins reveal their trafficking in live cells. *Nat. Commun.* **8**, 570 (2017).
49. S. Plantman *et al*., Integrin-laminin interactions controlling neurite outgrowth from adult DRG neurons in vitro. *Mol. Cell. Neurosci.* **39**, 50–62 (2008).
50. K. J. Tomaselli *et al*., Expression of beta 1 integrins in sensory neurons of the dorsal root ganglion and their functions in neurite outgrowth on two laminin isoforms. *J. Neurosci.* **13**, 4880–4888 (1993).
51. W. Wallquist *et al*., Dorsal root ganglion neurons up-regulate the expression of laminin-associated integrins after peripheral but not central axotomy. *J. Comp. Neurol.* **480**, 162–169 (2004).
52. N. Hoyer *et al*., Ret and substrate-derived TGF-β Maverick regulate space-filling dendrite growth in Drosophila sensory neurons. *Cell Rep.* **24**, 2261–2272.e5 (2018).
53. P. Soba *et al*., The Ret receptor regulates sensory neuron dendrite growth and integrin mediated adhesion. *eLife* **4**, e05491 (2015).
54. J. G. Cockburn, D. S. Richardson, T. S. Gujral, L. M. Mulligan, RET-mediated cell adhesion and migration require multiple integrin subunits. *J. Clin. Endocrinol. Metab.* **95**, E342–E346 (2010).
55. M. R. Andrews *et al*., Axonal localization of integrins in the CNS is neuronal type and age dependent. *eNeuro* **3**, ENEURO.0029-16.2016 (2016).
56. R. Eva *et al*., ARF6 directs axon transport and traffic of integrins and regulates axon growth in adult DRG neurons. *J. Neurosci.* **32**, 10352–10364 (2012).
57. R. Eva *et al*., Rab11 and its effector Rab coupling protein contribute to the trafficking of beta 1 integrins during axon growth in adult dorsal root ganglion neurons and PC12 cells. *J. Neurosci.* **30**, 11654–11669 (2010).
58. E. H. Franssen *et al*., Exclusion of integrins from CNS axons is regulated by Arf6 activation and the AIS. *J. Neurosci.* **35**, 8359–8375 (2015).
59. E. Vecino, J. P. Heller, P. Veiga-Crespo, K. R. Martin, J. W. Fawcett, Influence of extracellular matrix components on the expression of integrins and regeneration of adult retinal ganglion cells. *PLoS One* **10**, e0125250 (2015).
60. E. Gornstein, T. L. Schwarz, The paradox of paclitaxel neurotoxicity: Mechanisms and unanswered questions. *Neuropharmacology* **76**, 175–183 (2014).
61. B. G. Bober, E. Gutierrez, S. Plaxe, A. Groisman, S. B. Shah, Combinatorial influences of paclitaxel and strain on axonal transport. *Exp. Neurol.* **271**, 358–367 (2015).
62. V. Das, D. A. Sim, J. H. Miller, Effect of taxoid and nontaxoid site microtubule-stabilizing agents on axonal transport of mitochondria in untransfected and ECFP-htau40-transfected rat cortical neurons in culture. *J. Neurosci. Res.* **92**, 1155–1166 (2014).
63. N. E. LaPointe *et al*., Effects of eribulin, vincristine, paclitaxel and ixabepilone on fast axonal transport and kinesin-1 driven microtubule gliding: Implications for chemotherapy-induced peripheral neuropathy. *Neurotoxicology* **37**, 231–239 (2013).
64. T. Nakata, H. Yorifuji, Morphological evidence of the inhibitory effect of taxol on the fast axonal transport. *Neurosci. Res.* **35**, 113–122 (1999).
65. C. Theiss, K. Meller, Taxol impairs anterograde axonal transport of microinjected horseradish peroxidase in dorsal root ganglia neurons in vitro. *Cell Tissue Res.* **299**, 213–224 (2000).
66. I. Bobylev *et al*., Paclitaxel inhibits mRNA transport in axons. *Neurobiol. Dis.* **82**, 321–331 (2015).
67. A. Arjonen, J. Alanko, S. Veltel, J. Ivaska, Distinct recycling of active and inactive β1 integrins. *Traffic* **13**, 610–625 (2012).
68. M. Roberts, S. Barry, A. Woods, P. van der Sluijs, J. Norman, PDGF-regulated rab4-dependent recycling of alphavbeta3 integrin from early endosomes is necessary for cell adhesion and spreading. *Curr. Biol.* **11**, 1392–1402 (2001).
69. M. A. Nolte, E. N. M. Nolte-'t Hoen, C. Margadant, Integrins control vesicular trafficking; new tricks for old dogs. *Trends Biochem. Sci.* **46**, 124–137 (2020).
70. J. Chang, S. Lee, C. Blackstone, Spastic paraplegia proteins spastizin and spatacsin mediate autophagic lysosome reformation. *J. Clin. Invest.* **124**, 5249–5262 (2014).
71. A. C. Fernandes *et al*., Reduced synaptic vesicle protein degradation at lysosomes curbs TBC1D24/sky-induced neurodegeneration. *J. Cell Biol.* **207**, 453–462 (2014).
72. J. Sellin *et al*., Characterization of *Drosophila Saposin-related* mutants as a model for lysosomal sphingolipid storage diseases. *Dis. Model. Mech.* **10**, 737–750 (2017).
73. N. T. Sweeney, J. E. Brenman, Y. N. Jan, F. B. Gao, The coiled-coil protein shrub controls neuronal morphogenesis in Drosophila. *Curr. Biol.* **16**, 1006–1011 (2006).
74. V. Uytterhoeven, S. Kuenen, J. Kasprowicz, K. Miskiewicz, P. Verstreken, Loss of skywalker reveals synaptic endosomes as sorting stations for synaptic vesicle proteins. *Cell* **145**, 117–132 (2011).
75. M. S. Roberts, A. J. Woods, T. C. Dale, P. Van Der Sluijs, J. C. Norman, Protein kinase B/Akt acts via glycogen synthase kinase 3 to regulate recycling of alpha v beta 3 and alpha 5 beta 1 integrins. *Mol. Cell. Biol.* **24**, 1505–1515 (2004).
76. H. S. Hamid *et al*., Hyperglycemia- and neuropathy-induced changes in mitochondria within sensory nerves. *Ann. Clin. Transl. Neurol.* **1**, 799–812 (2014).
77. W. R. Kennedy, G. Wendelschafer-Crabb, T. Johnson, Quantitation of epidermal nerves in diabetic neuropathy. *Neurology* **47**, 1042–1048 (1996).
78. M. A. Khoshnoodi *et al*., Longitudinal assessment of small fiber neuropathy: Evidence of a non-length-dependent distal axonopathy. *JAMA Neurol.* **73**, 684–690 (2016).
79. M. Polydefkis *et al*., Reduced intraepidermal nerve fiber density in HIV-associated sensory neuropathy. *Neurology* **58**, 115–119 (2002).
80. M. T. Tseng *et al*., Skin denervation and cutaneous vasculitis in systemic lupus erythematosus. *Brain* **129**, 977–985 (2006).
81. B. Nieuwenhuis, B. Haenzi, M. R. Andrews, J. Verhaagen, J. W. Fawcett, Integrins promote axonal regeneration after injury of the nervous system. *Biol. Rev. Camb. Philos. Soc.* **93**, 1339–1362 (2018).
82. N. Majithia *et al*., National Cancer Institute-supported chemotherapy-induced peripheral neuropathy trials: Outcomes and lessons. *Support. Care Cancer* **24**, 1439–1447 (2016).
83. National Research Council, *Guide for the Care and Use of Laboratory Animals* (National Academies Press, Washington, DC, ed. 8, 2011).